Molecular BioSystems

RSC Publishing

PAPER

Chemical and biosynthetic evolution of the antimycin-type depsipeptides†

Cite this: *Mol. BioSyst.*, 2013, **9**, 2712

Stephanie A. Vanner,‡[ab] Xiang Li,‡[ab] Rostyslav Zvanych,[ab] Jonathon Torchia,[ab] Jing Sang,§[b] David W. Andrews§[b] and Nathan A. Magarvey*[ab]

Received 7th June 2013,
Accepted 16th August 2013

DOI: 10.1039/c3mb70219g

www.rsc.org/molecularbiosystems

Evolution of natural products, and particularly those resulting from microbial assembly line-like enzymes, such as polyketide (PK) and nonribosomal peptides (NRP), has resulted in a variety of pharmaceutically important and chemically diverse families of molecules. The antimycin-type depsipeptides are one such grouping, with a significant level of diversity and members that have noted activities against key targets governing human cellular apoptosis (*e.g.* Bcl-xL and GRP78). Chemical variance originates from ring size, with 9-, 12-, 15-, and 18-membered classes, and we show that such distinctions influence their molecular targeting. Further, we present here a systematic interrogation of the chemistry and assembly line evolution of antimycin-type analogues by conducting metabolomic profiling and biosynthetic gene cluster comparative analysis of the depsipeptide assembly lines for each member of the antimycin-group. Natural molecular evolution principles of such studies should assist in artificial re-combinatorializing of PK and NRP assembly lines.

1 Introduction

Microbial natural products, and particularly those with biosynthetic origins arising from polyketide synthase (PKS) and nonribosomal peptide synthetase (NRPS) assembly line-like enzymes, are noted for their chemical and functional diversity. Genetic and biochemical analyses often suggest that the numbers of combinations and permutations plausible from PK and NRP assembly line syntheses far exceeds the number of products present and isolated in a laboratory setting.[1] Directed re-design of these modular assemblages, known as combinatorial biosynthesis, assists in realizing unnatural products with improved/altered functionalities and pharmacophores.[2] The suite of NRPS and PKS machinery is comprised of a vast number of enzymatic domains and modules, with distinct monomer block selectivities (>500 for NRPSs and PKSs), and tailoring actions. Our ability to leverage this large repertoire of enzymatic machinery for combinatorial biosynthesis would, however, benefit significantly from an appreciation of how systems have already been combinatorialized in nature.[3] More specifically, to appreciate how natural evolution of assembly systems occurs may provide a framework to deploy re-engineering technologies. Furthermore, in several instances laboratory engineered re-fusions of natural product assemblies have resulted in non-functional recombinant assembly lines, undesired combined products or nearly negligible yields of the desired hybrid natural product. Unfortunately, only recent investigation into the more critical communication elements and domains (*e.g.* docking domains)[4] have led to an appreciation of molecular principles that enable natural interactions between modules and assembly line components. Moreover, most of the known biosynthetic gene clusters have been investigated with a focus on the functions of enzymes in their native assembly-line setting rather than on attempting to reveal the natural evolutionary principles that promote successful assembly line alteration or modification.[3] One means to gain access to accepted fusion and alteration points within assembly lines is to reveal divergence within evolutionarily related metabolites and their associated biosynthetic pathways. Retro-biosynthetic analyses, in combination with exhaustive interrogation of NRPS/PKS derived chemical diversity, may provide evidence for how nature itself evolved assembly lines.

Among these naturally selected molecular families, the antimycin-type depsipeptides are uniquely interesting with

[a] *Department Chemistry & Chemical Biology, McMaster University, M.G. DeGroote Institute for Infectious Disease Research, 1200 Main St. W, Hamilton, Ontario L8N 3Z5, Canada. Tel: +1 905 5259140 ext 22188*

[b] *Department of Biochemistry & Biomedical Sciences, McMaster University, M.G. DeGroote Institute for Infectious Disease Research, 1200 Main St. W, Hamilton, Ontario L8N 3Z5, Canada. E-mail: magarv@mcmaster.ca; Tel: +1 905 5259140 ext 22244*

† Electronic supplementary information (ESI) available: Mauve alignment of the 4 clusters and NMR data for all isolated compounds. See DOI: 10.1039/c3mb70219g

‡ These authors contributed equally to this work and are considered co-first authors.

§ Current address: Department of Biochemistry, University of Toronto, Sunnybrook Research Institute, 2075 Bayview Avenue, Toronto, Ontario M4N 3M5, Canada. E-mail: david.andrews@sri.utoronto.ca; Tel: +1 416-480-5120.

sequential macrolactone ring expansions engendering diverse anticancer activities. The most well recognized member of the group is the 9-membered antimycin and its related 9-membered congeners (*e.g.* UK-2A).[5,6] Functionally, this class is noted for its ability to act as a peptidomimetic and block the interaction between BH3-containing peptides and Bcl-xL.[7–9] Although, not completely understood, the interaction of antimycin with Bcl-xL is not dictated by the 2-hydroxy within the formamidosalicylic acid unit, as methylation does little to affect its targeted activity.[7,8] Methylation does, however, blunt the other noted interaction of the antimycins, and more specifically their binding and inhibition of NADH oxidase in the mitochondrial electron transport at complex III.[7,10] Moreover, the interactions of antimycin with the BH3 groove are seemingly not a common feature of the 12-, 15-, and 18-membered ring-expanded classes of the antimycins (Fig. 1). The 'ring-expanded' antimycins, JBIR-06 (12-membered) and prunustatin A (15-membered), however are noted for different activity that relates to eukaryotic cell death pathways, more specifically down-regulating the expression of GRP-78, a key component of the unfolded protein response.[11,12] As such, each of these various macrocyclic natural products are leads for this second anti-apoptotic pathway, up-regulated in numerous cancer cell subtypes. The antimycin-type depsipeptide family is further extended by an 18-member, respirantin, whose target is not yet known, but testing reveals a nanomolar inhibition profile of prostate cancer cell types.[13,14] The bioactivity interest in the antimycin-type series and its relationship to ring size and potentially other structural variations, presents a direct opportunity to analyze the evolution of a NRP-PK assembly line from a chemical and biological perspective. In the present study, we isolated 16 depsipeptides from *Streptomyces* sp. ADM21, *Streptomyces* sp. ML55 and *Streptoverticillium orinoci* (Fig. 2B) to assist in our appreciation of the spectrum of agents possible from their assembly lines. To further understand the structure–activity relationships (SAR) at play within and across the classes we tested a selection from the three groups of antimycin-type depsipeptides for Bcl-xL inhibition, demonstrating that only the 9-membered antimycins disrupted the Bcl-xL–BH3 interaction and interestingly, antimycin side chain length influences activity. Moreover, we present a detailed inspection of the assembly lines for the 4 antimycin-type ring classes to gain an appreciation of how nature drives its own combinatorial processes in order to inform possible future synthetic combinatorial studies.

2 Methods

2.1 General

^{1}H and ^{13}C NMR spectra were recorded on a Bruker AVIII 700 MHz NMR spectrometer using TMS as an internal standard. Chemical shifts (δ) expressed in parts per million (ppm) and coupling constants (J) are reported in Hertz (Hz). High resolution MS spectra were collected on a Thermo LTQ OrbiTrap

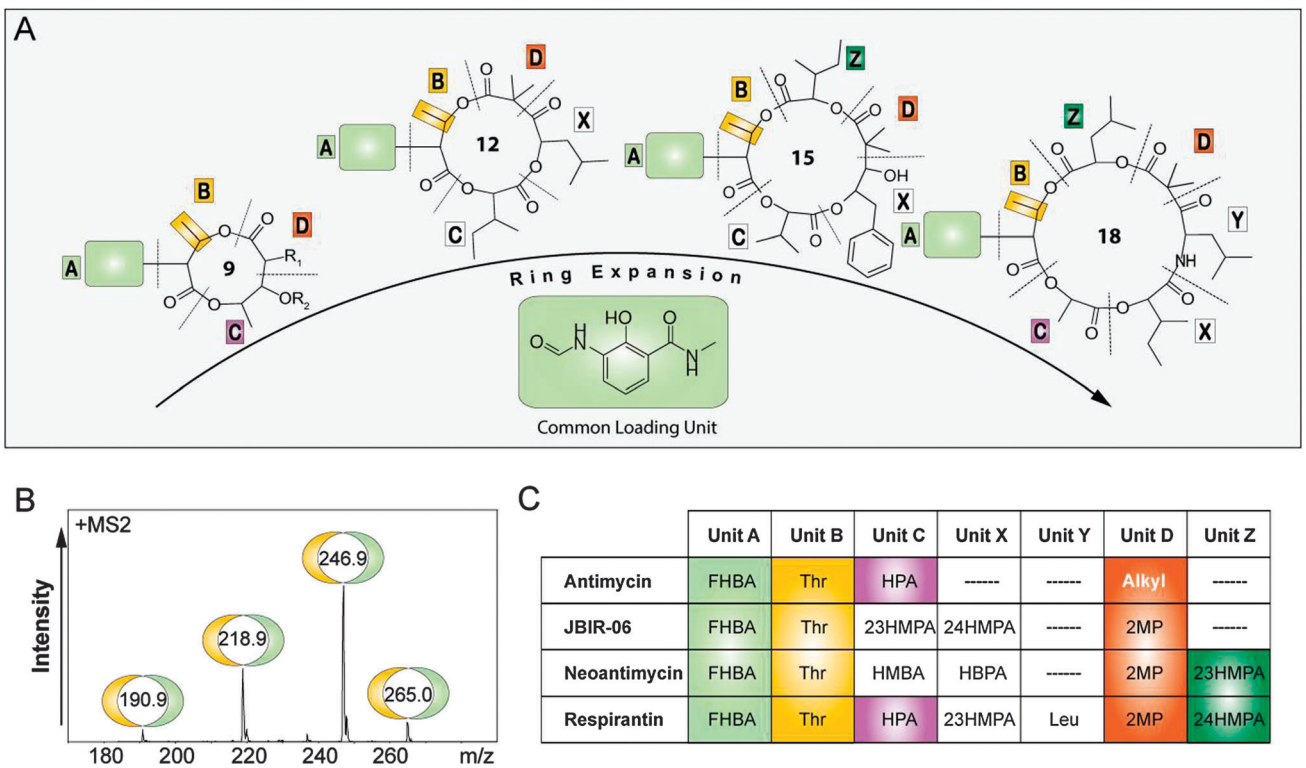

C

	Unit A	Unit B	Unit C	Unit X	Unit Y	Unit D	Unit Z
Antimycin	FHBA	Thr	HPA	------	------	Alkyl	------
JBIR-06	FHBA	Thr	23HMPA	24HMPA	------	2MP	------
Neoantimycin	FHBA	Thr	HMBA	HBPA	------	2MP	23HMPA
Respirantin	FHBA	Thr	HPA	23HMPA	Leu	2MP	24HMPA

Fig. 1 The 4 naturally occurring antimycin-type depsipeptides. (A) Each class is defined by divergent ring sizes to include 9-membered, 12-membered, 15-membered and 18-membered lactone macrocycle cores. Antimcyin R_1: $(CH_2)_5CH_3$, R_2: $COCH_2CH(CH_3)_2$. (B) Screening strategy for identification of antimycin-type analogues based on diagnostic MS/MS fragmentation pattern of units A and B common across all subtypes. (C) Description of antimycin-type depsipeptide units A-Y FHBA: 3-formamido-2-hydroxybenzoic acid, Thr: threonine, HPA: 2-hydroxypropanoic acid, 23HMPA: 2-hydroxy-3-methylpropanoic acid, HMBA: 2-hydroxy-3-methylbutanoic acid, 24HMPA: 2-hydroxy-4-methylpropanoic acid, HBPA: α-hydroxy-benzenepropanoic acid, Leu: leucine, 2MP: 2-methylpropanal.

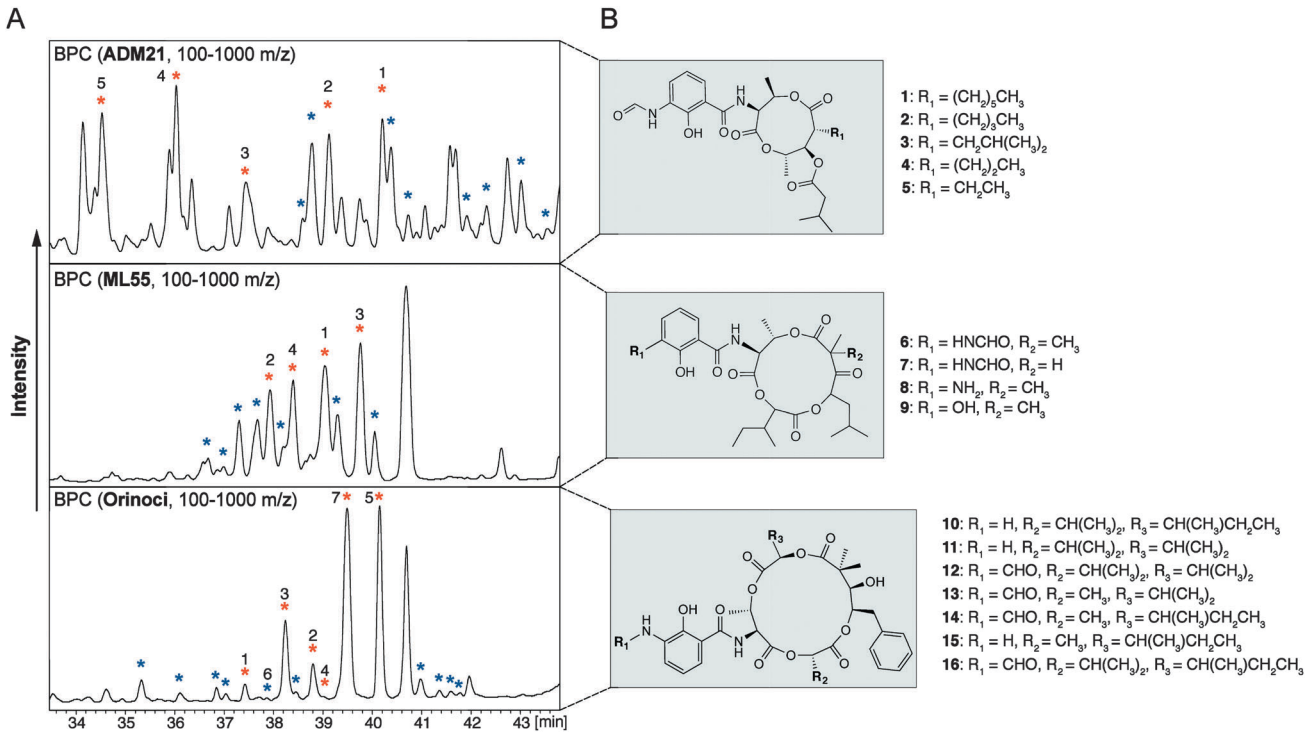

Fig. 2 Chemical diversity profiling from antimycin-type depsipeptide assembly lines from strains *Streptomyces* sp. ADM21, *Streptomyces* sp. ML55 and *Streptoverticillium orinoci*. (A) Base peak chromatograms from the extracts of the 3 depsipeptide producers. Stars highlight the peaks which exhibited MS/MS fragmentation corresponding to the antimycin-type diagnostic mass fragmentation pattern, refer to Fig. 1B. Orange stars indicate the peaks, and corresponding compounds that were isolated. (B) The structures of the purified compounds, consistent with the orange starred chromatogram peaks.

XL mass spectrometer (ThermoFisher Scientific, USA) with an electrospray ionization source (ESI) and using CID with helium for fragmentation. LC-MS data was collected using a Bruker Amazon-X ion trap mass spectrometer coupled with a Dionex UltiMate 3000 HPLC system, using a Luna C-18 column (250 mm × 4.6 mm, Phenomenex) for analytical separations, running acetonitrile and H_2O as the mobile phase. Column chromatography was carried out with silica gel (200–300 mesh), TLC: silica gel plates (Macherey-Nagel, SilG/UV254, 0.20 mm), spots were detected using the anisaldehyde reagent; Sephadex LH-20 was supplied by GE Health Co.

2.2 Extraction and isolation

5 mL of *Streptomyces* sp. ADM21 (kindly provided by Dr Harmit Laatsch, Georg-August-Universität Göttingen, Germany), *Streptomyces* sp. ML55 (kindly provided by Dr Shin-ya Kazuo, BIRC, Japan) and *Streptoverticiullium orinoci* (DSM 40571) seed were inoculated into 12 × 2.8 L Erlenmeyer flask containing 1 L culture medium consisting of glucose 4 g, yeast extract 4 g, malt extract 10 g and cultured at 28 °C for 4 days on a rotary shaker at 160 rpm. Fermentation was concentrated and chromatographed on a Sephadex LH-20 column and eluted with MeOH. Individual fractions were purified by semi-prep HPLC with gradient MeOH–H_2O (5% to 100%) as a mobile phase to yield the pure compounds (**1–16**).

2.3 Bcl-xL inhibition assays

Bcl-xL inhibits membrane permeabilization by the pro-apoptotic proteins cBid and Bax.[9] To measure the effects of the antimycin-type depsipeptides on the activity of Bcl-xL we measured the increase in fluorescence due to the release of the fluorophore/quencher pair 8-aminonaphthalene 1,3,6-trisulfonic acid (ANTS)/*p*-xylene-bis-pyridinium (DPX) from liposomes.[15] In this assay single addition of recombinant Bax (100 nM) or cBid (20 nM) to liposomes had little effect, but in combination the two proteins caused an increase in fluorescence due to membrane permeabilization that was inhibited by Bcl-xL (40 nM). Addition of antimycin-type depsipeptides that inhibited Bcl-xL restored the increase in fluorescence due to membrane permeabilization.

2.4 Genome sequencing and assembly

The *Streptomyces*' genomic DNA were isolated using standard phenol : chloroform extraction methods.[16] Briefly, *Streptomyces* sp. mycelia were resuspended in SET buffer (75 mM NaCl, 25 mM EDTA pH 8.0, 20 mM Tris-HCl pH 7.5) and treated with 1 mg mL^{-1} lysozyme for 60 minutes at 37 °C. After incubation, proteinase K was added to a concentration of 0.5 mg mL^{-1} and SDS to a concentration of 1%, and incubated at 55 °C for 2 hours. After incubation, the solution was brought to a final NaCl concentration of 1.25 M before extracting 3 times with 1 : 1 phenol chloroform buffered with Tris-HCl pH 8.0. After separating the organic and aqueous phase by centrifugation at 4500*g*, DNA was precipitated with 0.6 volume of isopropanol, and desalted with 70% ethanol. After drying, the DNA was resuspended in TE buffer. DNA samples were prepared using the Illumina protocol (TruSeq DNA Sample Preparation Guide, #15005180) and were

fragmented. The DNA fragment ends were repaired and phosphorylated using Klenow T4 DNA polymerase and T4 Polynucleotide Kinase. After purified the ligation product and PCR amplification, the library was validated and sequenced on the Illumina Hiseq 2000 using 100 bp PE processing. Sequence reads obtained, with ~50× coverage, were assembled into contigs using an Abyss genome sequence assembler. The gaps were filled with PCR using primers listed in Table S1 (ESI†).

2.5 Sequence and Mauve alignments and phylogenetic analysis

Nucleotide sequences were aligned using the Geneious R6 program, with default parameter settings (gap opening penalty, 10; gap extension penalty, 0.05; gap separation penalty range, 8; identity for alignment delay, 40%). The phylogenetic tree was constructed using the neighbor-joining algorithm with Geneious R6 with a gap penalty of 7 and gap extension penalty of 3. A Mauve alignment was performed using Geneious R6 progressive Mauve algorithm with a match seed weight of 20 and a minimum LCB score of 69.

3 Results and discussion

3.1 Chemical profiling of the antimycin-type chemical diversity

A chemical analysis of the antimycin-type depsipeptides was first conducted to profile the existing diversity across the 9-, 12-, 15- and 18-membered subtypes (Fig. 1A). The respective depsipeptides under study include the producers of each ring class, antimycin (9-membered), JBIR-06 (12-membered), neoantimycin (15-membered), and respirantin (18-membered).[6,11,13,17] To facilitate the recognition of structural similarities and the discrimination of differences between the 4 classes, unit names have been assigned to each monomer component in the equivalent position to those across the counterpart ring subtypes (Fig. 1C). The loading unit, 3-formamido-2-hydroxybenzoic acid (FHBA), unit A, and threonine (Thr), unit B, are common among all classes. Antimycin and respirantin include 2-hydroxy-propanoic acid (HPA) as unit C, whereas 2-hydroxy-3-methylpentanoic acid (23HMPA) in JBIR-06 and a 2-hydroxy-3-methylbutanoic acid (HMBA) in neoantimycin occupy this structural location. Unit X, not present in antimycin, is 2-hydroxy-4-methylpentanoic acid (24HMPA) in JBIR-06, α-hydroxy-benzenepropanoic acid (HBPA) in neoantimycin and 23HMPA in respirantin. There is a unique second amino acid component in respirantin, assigned as a unit Y, which is a leucine (Leu). Unit D of JBIR-06, neoantimycin, and respirantin, is a 2-methylpropanal component (2MP), which originates from a carboxylic acid bearing a gem-dimethyl (GDM) substituent. Conversely, unit D of antimycin is composed of variants with longer straight and branched alkyl chains. Respirantin and neoantimycin are further distinguished by an additional 24HMPA and 23HMPA α-keto acid constituent respectively, designated as unit Z (Fig. 1C).

To gain further insight into the types of structural variety nature elicits from the antimycin-type depsipeptides respective biosynthetic pathways, an MS/MS screening strategy was developed for analogue isolation. The specific positions of structural diversity, conferred by assembly line flexibility, within each ring subtype was then easily identified. In many instances a biosynthetic assembly line will create a number of variants that are co-produced with the dominant natural product.[18] Analogues not only serve to reveal SAR, but can also be used to illuminate the promiscuous properties of a biosynthetic assembly line.[18] Advanced screening from a number of natural product producers has shown that the variations of depsipeptides are particularly numerous. Isolation and characterization of 18 analogues of the broad-spectrum antitumour depsipeptide, cryptophycin, is a noteworthy example.[19] Often within natural product families, the greatest structural diversity arises from the incorporation of different monomer building blocks during biosynthesis, as opposed to post-assembly line modifications. As such we devised a strategy that would be capable of identifying members based on a general diagnostic fragmentation pattern from each ring-size class. First, the known antimycin, JBIR-06 and neoantimycin diagnostic fragments were established, *m*/*z* at 190.9, 218.9, 246.9 and 265.0 (Fig. 1B). Less abundant peaks in the chromatogram, sharing the signature fragmentation pattern, were subsequently isolated (Fig. 2A). This approach rapidly led to the identity of 5 antimycin variants, 4 JBIR-06 and 7 neoantimycin analogues, all of which have been previously characterized (Li, unpublished data).[6,11,17,20,21] Unfortunately, due to the distinct growing conditions of the respirantin producer, unrepeatable in a laboratory setting, we lacked sufficient material to purify analogues (data not shown). Structures of the 16 isolated compounds were confirmed by LC-MS/MS, 1D & 2D nuclear magnetic resonance (NMR) and by correlation of the spectral data to literature values (Fig. S1, ESI†).[11,17]

It is apparent from the sites of structural deviation across the subtypes and rich diversity of monomer building blocks within each subtype, that nature's antimycin-type assembly lines exhibit broad enzymatic flexibility (Fig. 2B). All five antimycin analogues (**1–5**), and one of the JBIR-06 analogues (**7**) differed in unit D. The antimycins contained varying alkyl chain tail lengths from three carbons, up to six in length and also an iso-butyl group, whereas one of the gem-dimethyl alkyl groups in JBIR-06 was replaced by hydrogen. Analogues of JBIR-06 and neoantimycin were both found to vary in unit A, in which the formamido group (**6** and **7**) was replaced by an amine (**5**) or hydroxyl group (**9**) in JBIR-06 and a hydrogen (**10**, **11**, and **15**) or formyl group (**12**, **13**, **14** and **15**) in neoantimycin. Rich chemical diversity is found amongst the neoantimycins in particular, with deviations occurring additionally at units C and Z. The differing α-keto acid building blocks include those with an isopropyl moiety (**10**, **11**, **12**, and **16**), or a methyl group (**13**, **14** and **15**) for unit C and 2-methylbutyl (**10**, **14**, **15** and **16**), or an isopropyl moiety (**11**, **12**, and **13**) for unit Z. The isolation of 16 analogues reflects the promiscuity of the unit A loading module, the unit D PKS module, and the α-keto acid loading units C and Z within the antimycin-type assembly lines, suggesting where future modifications could be made to these molecules through natural incorporations.

3.2 Antimycin-type biosynthetic assembly lines

For comparative purposes and to uncover assembly line diversification within the antimycin-type depsipeptides, we conducted

genomic sequencing of the antimycin (*Streptomyces* sp. ADM21), JBIR-06 (*Streptomyces* sp. ML55), neoantimycin (*Streptoverticillium orinoci*), and respirantin (Alaskan *Kitasatospora* sp.) producers. 100 bp paired end libraries were constructed and DNA used for the HiSeq2000 sequencing protocol. Each genomic sequencing scan yielded approximately 325, 310, 380 and 450 Mbp of DNA sequence of which assemblies lead to 210, 176, 128 and 392 large contigs. Recently antimycin biosynthetic clusters have been revealed from several strains including, *Streptomyces* sp. S4, *S. ambofaciens* ATCC 23877, *S. albus* J1074, *Streptomyces* sp. NRRL 2288, and *S. blastmyceticus* NBRC 12747.[22,23] We therefore used the *Streptomyces* sp. S4 antimycin gene cluster as a seed to search for the homologous antimycin cluster within *Streptomyces* sp. ADM21. The search results, specifically using AntH and AntI, those that encode for unit A, produced only one possible candidate for the antimycin gene cluster, with a sequence similarity of 93.5%. Additionally, a Basic Local Alignment Search (BLAST) was performed on the 3 larger ring-sized subtype producers against *Streptomyces* sp. S4 to locate their depsipeptide clusters. Leads were identified with similarities of 72.3%, 71.0%, and 69.1% for the JBIR-06 (*S.* sp. ML55), neoantimycin (*S. oronoci*), and respirantin (Alaskan *Kitasatospora* sp.) clusters respectively. Extension from each of the homologs produced antimycin-like assembly lines. However, with increasing product ring size came a higher number of modules, with *S.* sp. ML55 (12-membered JBIR-06 producer) containing 5 modules, *S. orinoci* (15-memebered neoantimycin producer) 6 modules, and Alaskan *Kitasatospora* sp. (18-membered respirantin producer) 7 modules (Fig. 3). Sequence interrogation of these biosynthetic loci is in keeping with the anticipated co-linearity and coding for each of the respective antimycin-type depsipeptides. Identification of the candidate depsipeptide clusters provided a logical starting point to assess how the antimycin-type assembly lines diverge.

Threonine-loading unit B appears to be highly conserved across the 4 assembly lines, thus it was the point of departure for further investigation. A multiple pairwise alignment of the 4 unit Bs revealed high percent sequence identities for the expanded ring subtype producers to the *S.* sp. ADM21 antimycin cluster, with JBIR-06 (*Streptomyces* sp. ML55) at 79.2%, neoantimycin (*S. orinoci*) at 78.7%, and respirantin (Alaskan *Kitasatospora* sp.) at 76.7%, demonstrating the similarities in composition and arrangement of base pairs in the unit B encoding portion of all 4 clusters. A narrower focus on the unit B adenylation domains, responsible for substrate selection and ultimate product chemistry, corroborated said results.

Genetic similarity was further exhibited through phylogenetic analysis and adenylation domain sequence alignment of all adenylation domains present within the 4 depsipeptide assembly lines (Fig. 4A and Fig. S3B, ESI†). The unit B adenylation domains were found to have the highest percent sequence identity across all of the assembly line adenylation domains, ranging from 73.8–80.9%, and had the closest level of ancestry as indicated by their grouping

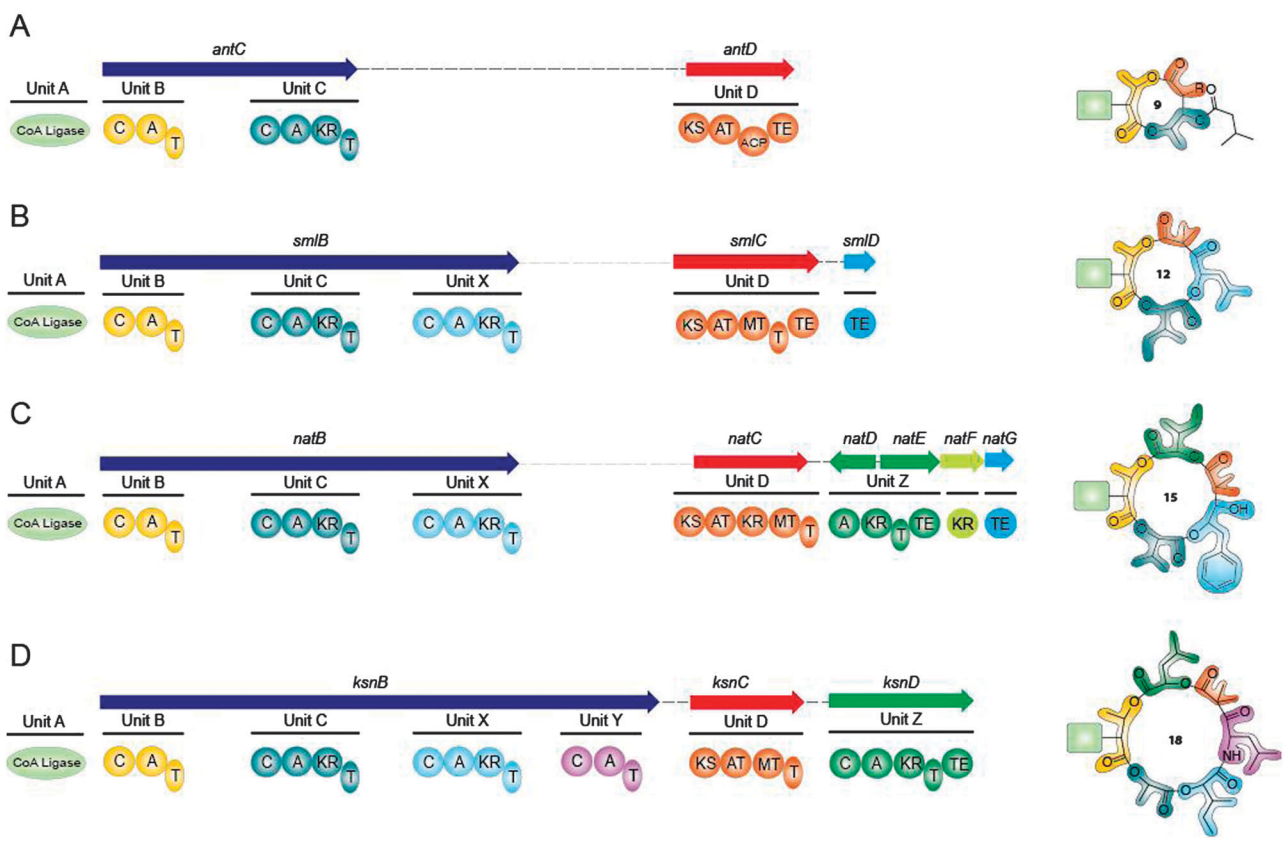

Fig. 3 The NRPS–PKS biosynthetic clusters that produce the 4 classes of antimycin-type depsipeptides.

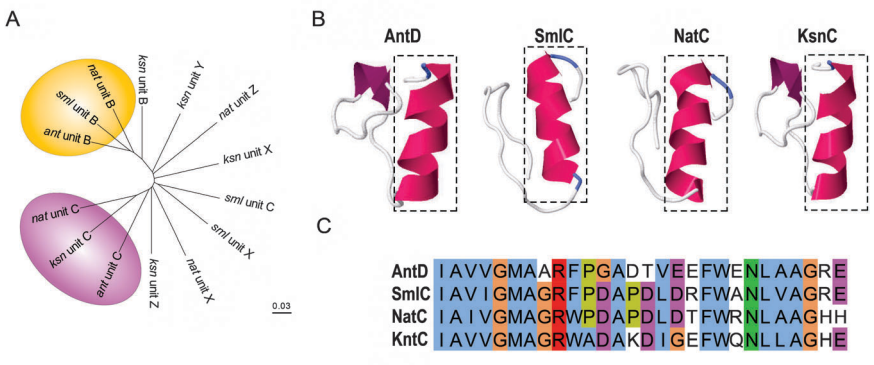

Fig. 4 (A) Phylogenetic analysis of the adenylation domains of the depsipeptides' biosynthetic clusters. (B) Simulated possible recognition/binding domain between the NRPS and PKS enzymes. (C) A 28 amino acid conserved domain representing a possible recognition/binding sequence between the NRPS and PKS enzymes.

in the phylogenetic tree. A protein level analysis of the unit B adenylation domains revealed that the substrate-selectivity governing amino acid sequence is highly conserved across the antimycin, JBIR-06, neoantimycin, and respirantin assembly lines, as indicated by the top line of amino acids in Fig. S3A (ESI†). These genetic and protein data, in hand with the chemical structural relationships of the depsipeptides, indicate as expected that *Streptomyces* sp. ADM21, *Streptomyces* sp. ML55, *S. orinoci*, and *Kitasatospora* sp., and consequently their products, antimycin, JBIR-06, neoantimycin and respirantin, evolved tangentially from a common route.

3.3 Bioinformatic investigation of assembly line relationships

Recognizing that the initiating units of the antimycin-type assembly lines are most likely derived from the same source led us to query how the genetic and consequent enzymatic insertions and extensions to assembly lines came about. It appears that there are three possible means by which highly structurally related families of natural products could arise from a common enzymatic root. The first means being through duplications of previous assembly line modules, the second by incorporation of novel DNA from the *same* bacterial source upon which point mutations could occur, and the third through the incorporation of novel DNA from *distinct* bacterial sources that leads to the greatest assembly line divergence. In the case of the three unit Xs, they do not appear to be duplications of unit Cs. The loaded α-keto acids are distinct and a multiple pairwise alignment of all 4 unit C and the 3 unit X sequences yielded relatively low sequence similarities between the C and X units, ranging from 57.3–64.7%. Moreover, it does not seem likely that the JBIR-06, neoantimycin and respirantin producers have incorporated this new unit from the same source, as the alignment produced sequence identities spanning from 58.9–65.7% for the 3 unit Xs. Further probing of the adenylation domain similarities showed that unit X of the respirantin producer is almost certainly an addition from a disparate source, with low sequence identity to that of the JBIR-06 and neoantimycin producers and diverging as its own branch in a phylogenetic analysis (Fig. 4A). The unit X origins for JBIR-06 and neoantimycin remain unclear, however, with an adenylation domain sequence identity of 68.5% and a close phylogenetic grouping (Fig. S3A, ESI† and Fig. 4A).

An alignment of the additional C-A-T module, unit Y, nucleotide sequence from the respirantin assembly line was performed with those of the 4 unit Bs, the conserved threonine-loading C-A-T found in all assembly lines, to provide insight on whether the distinctive unit is derived from a module duplication. The percent sequence identities are notably lower for the relationship between those encoding unit Y and the unit Bs (59.5–61.9%) than across the unit Bs (75.0–78.4%) from the different depsipeptide producers, suggesting that the unit Y sequence was integrated from an unrelated source. Further investigation was performed through a focus on the adenylation domains. A multiple alignment of the 4 unit B adenylation domains with the Y adenylation domain demonstrated that the unit Y adenylation domain is only 66.4–66.7% similar to those of the 4 unit Bs, whereas the unit Bs are 77.7–83.5% similar. Furthermore, the amino acid sequence governing substrate incorporation in unit Y diverges from the conserved sequence of the unit Bs, as indicated by the bottom line of amino acids in Fig. S3A (ESI†), therefore substantiating that unit Y is not derived from an antimycin-type assembly line DNA replication.

We proceeded to investigate the relationship of unit Z to the other antimycin-type C-A-KR-T modules. The neoantimycin unit Z shares a sequence identity ranging from 51.0–56.2% with units C and X and the respirantin unit Z has a sequence identity of 55.7–59.5% to these same units upon performing a multiple alignment of all C, X, and Z units. The low homologies between the unit Z nucleotide sequences and those of previous C-A-KR-T modules, units C or X, suggest that they have not likely arisen through DNA duplication. The unit Z incorporations also appear to have come from different sources, as the sequence alignment produced a similarity of 53.7% between that from the neoantimycin and respirantin assembly lines.

A Mauve analysis was next performed to gain a more complete view of the genetic evolutionary relationships between the 4 full-length antimycin-type depsipeptide biosynthetic clusters (Fig. S4, ESI†). Mauve is a more sophisticated multiple

genome alignment program, capable of processing large-scale evolutionary events, including insertions and rearrangements.[24] It groups nucleotide sequences sharing ancestral roots by colour and the level of similarity is indicated by the intensity on the plot. The pink alignment component is suggestive that unit B is the same across the antimycin, JBIR-06, neoantimycin and respirantin assembly lines, further corroborating our previous computational homology investigations. It is interesting to note that module insertions do not appear to occur after T domains, but more likely around C domains as indicated by the alignment colour transitions from pink to green/red and yellow to red/green across the 4 assembly lines. Our examination yielded another definitive common sequence across the 4 antimycin-type clusters located at the beginning of the PKS modules (Fig. 4B), which we propose to be a conserved docking domain. A protein interaction that docks NRPS to PKS units must occur, but has been uncharacterized to date. Looking at the antimycin-type NRPS termini there are no clear sequence patterns that could partner a PKS docking domain, for recent structural studies have provided important new insights relating to the architecture and mechanism of type I PKS associations. By X-ray crystallographic analysis of the PikAIII/PikAIV docking domain interface, Buchholz *et al.* suggested α-helical regions are involved in protein–protein interaction between two PKS module.[4] An 80–100 amino acid sequence is known to be the docking component on the C′ terminus of the acyl carrier protein (ACP), with which a 30–40 N-terminal sequence of the ketosynthase (KS) interacts.[25] The identified conserved sequence in the antimycin-type assembly lines was 28 amino acids found near the N terminus of the KS domain. We, therefore, proceeded to generate 3D models of 4 PKS enzymes within each depsipeptide cluster based on reported PKS crystal structures (Fig. 4B). Each contains a conserved α-helical region at the very beginning of the sequence, which could potentially serve as an NRPS–PKS interaction surface. Although the question remains of how an NRPS specifically interacts with its PKS cognate, the data indicates another potential shared evolutionary trait of the 4 antimycin-type depsipeptides.

Next, we sought to further characterize the unit D PKS domains to unveil the divergences in substrate selectivity as the antimycin assembly line alone incorporates alkyl-chain containing monomers. We anticipated that the antimycin assembly line acyltransferase (AT) would be sufficiently different from ATs in the other systems, however a nucleotide alignment revealed a 66.4%, 67.5%, and 67.2% sequence similarity between the antimycin AT encoding DNA and that of JBIR-06, neoantimycin, and respirantin respectively. Moreover, a near identical conserved 13 amino acid sequence was predicted for the substrate-selecting domain of the AT in all 4 assembly lines (Fig. S5, ESI†), perhaps suggesting that site-specific mutations at other locations within the conserved acyltransferases are responsible for conferring different substrate selectivity. The ketosynthases are also relatively similar, with shared nucleotide identity of 71.9% (JBIR-06), 69.5% (neoantimycin), and 73.5% (respirantin) to the antimycin producer. Noted divergence occurs, however, after the AT, with insertions of ketoreductase (KR) and methyltransferase (MT) domains. It appears, therefore, that the conserved KS-AT di-domain is sufficiently hyper-variable to imbue antimycin with unique chemistry in comparison to the other ring subtypes. With knowledge of such KS-AT promiscuity, it is reasonable to propose rational future combinatorial manipulations that specifically leverage this unit D di-domain.

3.4 Bioactivity assessment of the antimycin-type depsipeptides

The differences within and across the antimycin-type ring classes begs the question, is the noted protein–protein blocking interaction of antimycin in keeping with the common unit A of all the subtype structures, or with one of the ancillary components? To probe this, we tested JBIR-06 and neoantimycin against the known inhibitor of BH3–Bcl-xL binding, antimycin 3A (Fig. 5B). The results of these experiments imply that the action of antimycin A3 in blocking BH3 binding is not exclusive to unit A. Furthermore, they are consistent with alterations to unit A in the methoxy antimycin series, which is a current clinical lead that exhibits no change in activity from antimycin A3.[7]

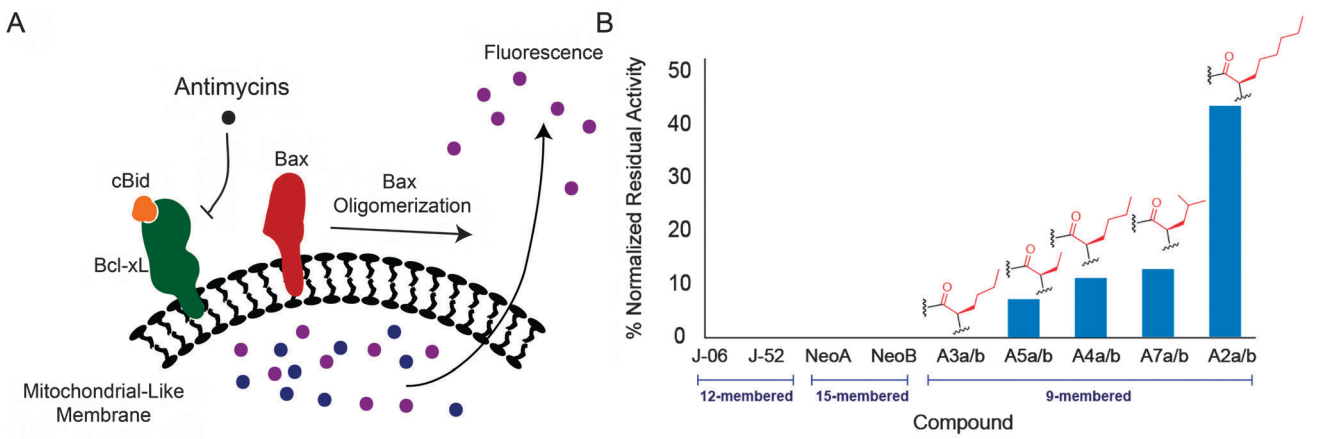

Fig. 5 (A) Schematic overview of fluorescent polarization Bcl-xL inhibition assay. (B) Inhibition of Bcl-xL by isolated compounds, J-06 (JB1R-06),[11] J-52 (JBIR-52),[20] NeoA (neoantimycin A),[17] NeoB (neoantimycin B)[26] and A2, A3, A4,[6] A5[27] and A7[28] represent antimycin 2, 3, 4, 5 and 7.

Our ability to profile the antimycin type depsipeptides led us to further query actions of the antimycin series exclusively. We isolated a variety of antimycin analogues with varying chain lengths in the fatty acid chain component, unit D, and found that the chain length is a driving factor for Bcl-xL inhibition (Fig. 5B). Antimycin A3a/b, 4 carbon alkyl chain, was not as active as the longer tailed variant antimycin A2a/b, a 6 carbon alkyl chain, which demonstrated the most potent activity and thus the importance of the alkyl component to Bcl-xL inhibition. Such systematic chemical profiling and bioactivity assessment not only shows the diversification enabled by the assembly lines, but also the molecular and functional uniqueness of independent members of the antimycin-type depispeptides.

4 Conclusions

In this work, we were able to interrogate the various structures of the antimycin-type depsipeptides from variant biosynthetic sources and reveal the assembly line machinery for each of the 9-, 12-, 15-, 18-membered ring subtypes. Through computational probing and comparison of their assembly lines, we generated a picture of how these biosynthetic machineries are related to one another. Furthermore, we have perhaps uncovered modules of promiscuity, one of which is the acyltransferase, unit D, as in the antimycin series it leads to the incorporation of substrates with varying fatty acid tails, where in other types loading is constrained to methylmalonate and malonate monomers. Investigations of chemical and biosynthetic evolution of natural assembly lines, such as this, may importantly create opportunities to appreciate how nature evolves assembly lines, which in turn may be useful and significant for future combinatorial biosynthetic efforts.

Acknowledgements

This work was supported by grant FRN106708 from Canadian Institutes of Health Research to NAM, Canada Research Chair, and by grant FRN12517 from the Canadian Institutes of Health Research to DWA. We thank Dr Shin-ya Kazuo (BIRC, Tokyo, Japan) for providing the *Streptomyces* ML55 strain and Robin Petitt and George Pettit (Department of Chemistry and Biochemistry, Arizona State University) for providing *Kitosatospora* sp.

References

1 S. Donadio, P. Monciardini and M. Sosio, *Nat. Prod. Rep.*, 2007, **24**, 1073–1109.
2 F. T. Wong and C. Khosla, *Curr. Opin. Chem. Biol.*, 2012, **1**, 117–123.
3 M. A. Fischbach and C. T. Walsh, *Chem. Rev.*, 2006, **106**, 3468.
4 T. J. Buchholz, T. W. Geders, F. E. Bartley III, K. A. Reynolds, J. L. Smith and D. H. Sherman, *ACS Chem. Biol.*, 2009, **4**, 41–52.
5 K. Tani, Y. Usuki, K. Motoba, K. Fujita and M. Taniguchi, *J. Antibiot.*, 2002, **55**, 315–321.
6 W. Liu and F. M. Strong, *J. Am. Chem. Soc.*, 1959, **81**, 4387–4390.
7 S. P. Tzung, K. M. Kim, G. Basañez, C. D. Giedt, J. Simon, J. Zimmerberg, K. Y. Zhang and D. M. Hockenbery, *Nat. Cell Biol.*, 2001, **3**, 183–191.
8 K. M. Kim, C. D. Giedt, G. Basañez, J. W. O'Neill, J. J. Hill, Y. H. Han, S. P. Tzung, J. Zimmerberg, D. M. Hockenbery and K. Y. J. Zhang, *Biochemistry*, 2001, **40**, 4911–4922.
9 S. Cory and J. M. Adams, *Nat. Rev. Cancer*, 2002, **2**, 647–656.
10 N. Tokutake, H. Miyoshi, T. Satoh, T. Hatano and H. Iwamura, *Biochim. Biophys. Acta*, 1994, **1185**, 271–278.
11 J. Y. Ueda, A. Nagai, M. Izumikawa, S. Chijiwa, M. Takagi and K. Shin-ya, *J. Antibiot.*, 2008, **61**, 241–244.
12 Y. Umeda, S. Chijiwa, K. Furihata, K. Furihata, S. Sakuda, H. Nagasawa, H. Watanabe and K. Shin-ya, *J. Antibiot.*, 2005, **58**, 206–209.
13 I. Urushibata, A. Isogai, S. Matsumoto and A. Suzuki, *J. Antibiot.*, 1993, **46**, 701–703.
14 G. R. Pettit, T. H. Smith, S. Feng, J. C. Knight, R. Tan, R. K. Pettit and P. A. Hinrichs, *J. Nat. Prod.*, 2007, **70**, 1073–1083.
15 J. A. Yethon, R. F. Epand, B. Leber, R. M. Epand and D. W. Andrews, *J. Biol. Chem.*, 2003, **278**, 48935–48941.
16 K. Smalla, N. Cresswell, L. C. Mendonca-Hagler, A. Wolters and J. D. van Elsas, *J. Appl. Bacteriol.*, 1993, **74**, 70–75.
17 G. Cassinelli, A. Grein, P. Orezzi, P. Pennella and A. Sanfilippo, *Arch. Mikrobiol.*, 1967, **55**, 358–368.
18 M. Nett, H. Ikeda and B. S. Moore, *Nat. Prod. Rep.*, 2009, **26**, 1362–1384.
19 T. Golakoti, J. Ogino, C. E. Heltzel, T. L. Husebo, C. M. Jensen, L. K. Larsen, G. M. L. Patterson, R. E. Moore and S. L. Mooberry, *J. Am. Chem. Soc.*, 1995, **117**, 12030–12049.
20 I. Kozone, J. Ueda, M. Takagi and K. Shin-ya, *J. Antibiot.*, 2009, **62**, 593–595.
21 Y. Takeda, T. Masuda, T. Matsumoto, Y. Takechi, T. Shingu and H. G. Floss, *J. Nat. Prod.*, 1998, **61**, 978–981.
22 M. Sandy, Z. Rui, J. Gallagher and W. Zhang, *ACS Chem. Biol.*, 2012, **7**, 1956–1961.
23 R. F. Seipke, J. Barke, C. Brearley, L. Hill, D. W. Yu, R. J. M. Goss and M. I. Hutchings, *PLoS One*, 2011, **6**, e22028.
24 A. E. Darling, T. J. Treangen, X. Messeguer and N. T. Perna, *Methods Mol. Biol.*, 2007, **396**, 135–152.
25 R. W. Broadhurst, D. Nietlispach, M. P. Wheatcroft, P. F. Leadlay and K. J. Weissman, *Chem. Biol.*, 2003, **10**, 723–731.
26 K. Takahashi, E. Tsuda and K. Kurosawa, *J. Antibiot.*, 2001, **54**, 867–873.
27 G. Schilling, D. Berti and D. J. Kluepfel, *J. Antibiot.*, 1970, **23**, 81–90.
28 C. J. Barrow, J. J. Oleynek, V. Marinelli, H. H. Sun, P. Kaplita, D. M. Sedlock, A. M. Gillum, C. C. Chadwick and R. Cooper, *J. Antibiot.*, 1997, **50**, 729–733.